Check for updates

AGU ADVANCING EARTH AND SPACE SCIENCES

Geophysical Research Letters

RESEARCH LETTER
10.1029/2026GL124043

Historical and Projected Antarctic Sea Ice Trends Across High-Resolution Coupled Model Hierarchies

Mitchell Bushuk[1], David B. Bonan[2,3], Stephen M. Griffies[4,5], William Gregory[5], Yongfei Zhang[6,5], Bill Hurlin[1], Yan-Ting Chen[5], Thomas Rackow[7], and Helge F. Goessling[8]

[1]National Oceanic and Atmospheric Administration/Geophysical Fluid Dynamics Laboratory, Princeton, NJ, USA, [2]Department of Atmospheric and Climate Science, University of Washington, Seattle, WA, USA, [3]Cooperative Institute for Climate, Ocean, and Ecosystem Studies, University of Washington, Seattle, WA, USA, [4]LOCEAN Laboratory, Sorbonne Université/CNRS/IRD/MNHN, Paris, France, [5]Atmospheric and Oceanic Sciences Program, Princeton University, Princeton, NJ, USA, [6]Now at Independent Researcher, [7]European Centre for Medium-Range Weather Forecasts, Bonn, Germany, [8]Alfred Wegener Institute, Helmholtz Centre for Polar and Marine Research, Bremerhaven, Germany

Key Points:

- Ocean and atmosphere model resolution show no clear influence on Antarctic sea ice trends across a suite of climate models
- The considered models with high ocean resolution show no evidence of a delayed sea ice decline relative to low-resolution counterparts
- Large amplitude, multi-decadal Southern Ocean internal variability is required to capture observed Antarctic sea ice extent trends

Supporting Information:

Supporting Information may be found in the online version of this article.

Correspondence to:

M. Bushuk,
mitchell.bushuk@noaa.gov

Citation:

Bushuk, M., Bonan, D. B., Griffies, S. M., Gregory, W., Zhang, Y., Hurlin, B., et al. (2026). Historical and projected Antarctic sea ice trends across high-resolution coupled model hierarchies. *Geophysical Research Letters*, *53*, e2026GL124043. https://doi.org/10.1029/2026GL124043

Received 29 APR 2026
Accepted 25 JUN 2026

Published 2026. This article is a U.S. Government work and is in the public domain in the USA. Geophysical Research Letters published by Wiley Periodicals LLC on behalf of American Geophysical Union.
This is an open access article under the terms of the Creative Commons Attribution License, which permits use, distribution and reproduction in any medium, provided the original work is properly cited.

Abstract Coupled climate models generally simulate a decline in Antarctic sea ice extent (SIE) over the satellite period, failing to capture the observed near-zero trend. Recent work has suggested that high-resolution ocean models could ameliorate this issue via improved representation of mesoscale ocean processes, which may delay simulated Antarctic SIE decline. We investigate this hypothesis using two high-resolution hierarchies of coupled climate models developed at GFDL and NCAR, which span atmospheric resolutions of 0.25°–1° and ice-ocean resolutions of 0.1°–1°, as well as three generations of Coupled Model Intercomparison Project (CMIP) models. Across the high-resolution hierarchies and CMIP ensembles, we find no clear relationship between ocean and atmospheric resolution and Antarctic SIE trends over both the satellite period and the remainder of the 21st century. Climate models that reproduce observed trends in individual ensemble members are those that exhibit large amplitude multi-decadal Southern Ocean climate variability.

Plain Language Summary Coupled climate models generally simulate a decline in Antarctic sea ice over the satellite period of 1979–2025, failing to capture the observed near-zero trend. Due to computational cost constraints, these models typically simulate the ocean and atmosphere using grid boxes of approximately 100 km scale and are unable to directly resolve ocean eddies. Recent work has suggested that high-resolution ocean models that explicitly resolve these ocean eddies and their associated impacts on heat exchanges within the climate system better simulate changes in Antarctic sea ice. We investigate this hypothesis using resolution hierarchies of climate models developed at two climate modeling centers, which include both high and low resolution model versions. We also consider three generations of Coupled Model Intercomparison Project (CMIP) climate models, which are generally low-resolution. Across the high-resolution hierarchies and CMIP ensembles, we find no clear relationship between ocean and atmosphere resolution and Antarctic SIE trends over both the satellite period and the remainder of the 21st century. The models that can occasionally reproduce observed sea ice extent trends exhibit large amplitude multi-decadal Southern Ocean climate variability.

1. Introduction

In contrast to the observed decline in Arctic sea ice extent (SIE), Antarctic sea ice exhibited an expansion over the period 1979–2014 (Fogt et al., 2022; Parkinson, 2019). This period of expansion was followed by a decade of striking sea ice loss, including several record-setting low-SIE years, leading some to suggest that Antarctic sea ice may have undergone a regime shift (Abram et al., 2025; Hobbs et al., 2024; Purich & Doddridge, 2023; Raphael et al., 2025). Climate models participating in Phases 5 and 6 of the Coupled Model Intercomparison Project (CMIP) generally simulate a decline of Antarctic SIE over the satellite period and fail to capture the observed trend (Roach et al., 2020; Shu et al., 2020; Turner et al., 2013). Holmes et al. (2024) showed that the inclusion of recent low SIE years brings the models into better agreement with observations; however, the observed near-zero trend remains near the edge of the model distribution. Additionally, models with trends similar to the observed fail to simulate the correct climatology and spatial and temporal variability of Antarctic sea ice (Roach & Polvani, 2026).

A number of hypotheses have been proposed to explain the inability of climate models to capture the observed Antarctic SIE trend. These include missing freshwater forcing associated with Antarctic ice sheet meltwater (Bronselaer et al., 2018; Schmidt et al., 2023), an underestimated shift in the Southern Hemisphere westerly wind jet and Southern Annular Mode (SAM; Ferreira et al., 2015; Purich, Cai, et al., 2016), natural multi-decadal variability of Southern Ocean deep convective cycles (Zhang et al., 2019), biased trends in surface winds and sea ice drift (Holland & Kwok, 2012; Sun & Eisenman, 2021), tropical SST variability and polar teleconnections associated with the Interdecadal Pacific Oscillation (Meehl et al., 2016; Purich, England, et al., 2016), biases in climatological ocean circulation and the associated delayed Southern Ocean warming (Armour et al., 2016), and internal climate variability (Polvani & Smith, 2013; Singh et al., 2019).

Another hypothesis recently put forward by Rackow et al. (2022) is that the low ocean resolution of many climate models, which is too coarse to directly resolve mesoscale ocean eddies, has systematically biased Antarctic sea ice trends. This hypothesis is based on a body of work demonstrating that mesoscale eddies play a crucial role in regulating the Southern Ocean response to climate change (Doddridge et al., 2019; Hallberg & Gnanadesikan, 2006; Hogg et al., 2008; Munday et al., 2013). Rackow et al. (2022) posited that explicitly resolving these eddies, and their associated impacts on Southern Ocean stratification, heat transport, and the meridional overturning circulation, will provide higher-fidelity Antarctic sea ice projections. Indeed, they found that a high-resolution climate model simulation had a delayed Antarctic sea ice decline relative to a low-resolution counterpart. Using an additional mixed-resolution simulation, they attributed the delayed sea ice decline to the use of high ocean resolution. Rackow et al. (2022) also found that higher-resolution CMIP5 models tended to simulate more accurate SIE trends than lower-resolution CMIP5 models.

Other prior results regarding the influence of high-ocean resolution on Southern Ocean sea ice and SST trends are equivocal. On one hand, the studies of Bilgen and Kirtman (2020), Yeager et al. (2023), and Kang et al. (2026) each showed improvements in Southern Ocean cooling in high-resolution models relative to their low-resolution counterparts. On the other hand, in a multi-model assessment of high-resolution models from HighResMIP (Haarsma et al., 2016), Dhame et al. (2025) showed that Southern Ocean SST trends are not systematically improved in high-resolution models. Similarly, Selivanova et al. (2024) found limited impacts of horizontal resolution on Antarctic sea ice trends across HighResMIP models. Bitz and Polvani (2012) found similar sea ice responses to stratospheric ozone depletion in both high-resolution and low-resolution ocean configurations. In ice-ocean simulations forced by atmospheric reanalysis, Chassignet et al. (2020) found similar Antarctic SIE trends between high ($\sim 0.1°$) and low ($\sim 1°$) ocean resolution models. It is notable that most of the HighResMIP models use a nominal 0.25° resolution, which is neither eddy-resolving (grid spacing <6.5 km) nor eddy-permitting (6.5 km < grid spacing < 13 km) over the Southern Ocean. The model considered in Rackow et al. (2022) is eddy-permitting only over the core of the Antarctic Circumpolar Current. Thus, it is crucial to examine higher-resolution models, which more fully represent high-latitude mesoscale eddy dynamics over the whole Southern Ocean.

In this work, we examine the impact of horizontal resolution on Antarctic SIE trends using two novel high-resolution hierarchies of coupled climate models, which include models that are eddy-permitting and eddy-resolving in the Southern Ocean, and models spanning several generations of CMIP. Models within each hierarchy share common model components and span atmospheric resolutions of 0.25°–1° and ice-ocean resolutions of 0.1°–1°, enabling a systematic investigation of the roles of oceanic and atmospheric resolution on Antarctic SIE trends. We also revisit the CMIP5-based findings of Rackow et al. (2022) using three generations of CMIP models, which span oceanic and atmospheric resolutions of 0.25°–4° and 0.5°–4°, respectively. Across these model suites, we find that Antarctic SIE trends do not exhibit clear relationships with oceanic or atmospheric resolution. We additionally argue that internal variability obscures structural resolution-dependent model differences and must be accounted for to make robust attribution statements.

2. Methods

2.1. GFDL High-Resolution Coupled Model Hierarchy

We analyze a resolution hierarchy of coupled climate models developed at the NOAA Geophysical Fluid Dynamics Laboratory (GFDL). The hierarchy consists of seven recently-developed coupled models, spanning ocean resolutions of 1/8°–1° and atmospheric resolutions of 25–100 km (see Table S1 in Supporting Information S1). The use of common model components across the hierarchy allows for a relatively clean study of the impacts of

19448007, 2026, 16, Downloaded from https://agupubs.onlinelibrary.wiley.com/doi/10.1029/2026GL124043, Wiley Online Library on [20/08/2026]. See the Terms and Conditions (https://onlinelibrary.wiley.com/terms-and-conditions) on Wiley Online Library for rules of use; OA articles are governed by the applicable Creative Commons License

10.1029/2026GL124043
19448007, 2026, 16, Downloaded from https://agupubs.onlinelibrary.wiley.com/doi/10.1029/2026GL124043, Wiley Online Library on [20/08/2026]. See the Terms and Conditions (https://onlinelibrary.wiley.com/terms-and-conditions) on Wiley Online Library for rules of use; OA articles are governed by the applicable Creative Commons License

horizontal resolution on emergent model simulation features. However, it is also important to note that the models differ in some model configuration choices. For example, the 1/2° and 1° ocean models employ a parameterization of mesoscale eddy effects, whereas the higher-resolution ocean models do not.

Each of the GFDL models is built from the same component models: the Atmosphere Model version 4 (AM4; Zhao et al., 2018a), the Land Model version 4 (LM4; Zhao et al., 2018a), the Modular Ocean Model version 6 (MOM6; Adcroft et al., 2019), and the Sea Ice Simulator version 2 (SIS2; Adcroft et al., 2019). Here, we summarize the resolution characteristics of the seven GFDL models considered in this study (see Table S1 in Supporting Information S1), and refer readers to the corresponding model documentation papers for further details. The CM4X models are the highest ocean resolution GFDL models considered in this study. CM4X-p125 and CM4X-p25 have 1/8° and 1/4° ocean-ice resolutions, respectively, and a common 50 km atmosphere-land resolution (Griffies et al., 2025a, 2025b). The CM4.0 model also employs a 1/4° ocean-ice resolution, but has a coarser 100 km resolution in the atmosphere-land components (Held et al., 2019). The ESM4.1 model utilizes a 1/2° ocean-ice resolution and a 100 km atmosphere-land resolution (Dunne et al., 2020). Finally, we consider three SPEAR models, SPEAR_LO, SPEAR_MED, and SPEAR_HI. Each of the SPEAR models has 1° ocean-ice resolution and atmosphere-land resolutions of 100, 50, and 25 km, respectively (Delworth et al., 2020). All seven models use 75 vertical ocean layers defined by the MOM6 hybrid vertical coordinate, which transitions from a geopotential-like coordinate in the upper ocean to isopycnal coordinates in the ocean interior. All models employ 33 atmospheric vertical levels except ESM4.1, which uses 49 levels for a better representation of stratospheric dynamics and chemistry.

We analyze Historical and SSP5-8.5 experiments performed with each model, following the CMIP6 forcing protocol which use Historical forcings over the period 1850–2014 and SSP5-8.5 scenario forcings over the period 2015–2100 (Eyring et al., 2016). Five of the GFDL models have ensembles of historical and scenario simulations, consisting of 30, 30, 10, 10, and 3 members for SPEAR_LO, SPEAR_MED, SPEAR_HI, CM4X-p25, and CM4.0, respectively. The other models considered (CM4X-p125 and ESM4.1) each have a single ensemble member.

2.2. NCAR High-Resolution Coupled Model Hierarchy

We also analyze a resolution hierarchy of models developed at the National Center for Atmospheric Research (NCAR). The hierarchy consists of high and low-resolution counterpart models based on the Community Earth System Model version 1.3 (CESM 1.3; Meehl et al., 2019; Chang et al., 2020; Castruccio et al., 2024). We refer to these models as CESM-HR and CESM-LR, respectively. The CESM-HR employs nominal resolutions of 1/10° for the ocean and sea ice and 1/4° for the atmosphere and land, whereas CESM-LR uses nominal 1° resolution across all components. Both models have 62 ocean vertical levels and 30 vertical levels in the atmosphere. As with the GFDL hierarchy, these CESM models share identical model components, but differ in some model configuration choices such as mesoscale and submesoscale eddy parameterizations (Chang et al., 2020). The component models used by CESM 1.3 are the Community Atmosphere Model version 5 (CAM5; Neale et al., 2012), the Parallel Ocean Program version 2 (POP2; Danabasoglu et al., 2012), the Community Ice Code version 4 (CICE4; Hunke et al., 2008), and the Community Land Model version 4 (CLM4; Lawrence et al., 2011).

We analyze Historical and RCP8.5 experiments performed with each model, following the CMIP5 forcing protocol which use Historical forcings over the period 1850–2005 and RCP8.5 scenario forcings over the period 2006–2100 (Meinshausen et al., 2011). Both CESM-HR and CESM-LR are run as 10-member ensembles of historical and scenario simulations.

2.3. CMIP3, CMIP5 and CMIP6 Models

We consider Antarctic SIE and sea ice area (SIA) from a suite of CMIP3, CMIP5, and CMIP6 models. For CMIP3, we analyze data from 18 models that were forced with CMIP3 historical forcing over the period 1850–1999 and SRESA1B scenario forcing over the period 2000–2100. For CMIP5, we analyze 39 models forced with CMIP5 historical forcing over the period 1850–2005 and RCP8.5 scenario forcing over the period 2006–2100. For CMIP6, we analyze 33 models forced with CMIP6 historical forcing over the period 1850–2014 and SSP5-8.5 scenario forcing over the period 2015–2100. Following Rackow et al. (2022), for CMIP models that submitted multiple ensemble members, we base our analysis on the ensemble mean for that model. Performing analyses that include each individual ensemble member does not change our qualitative findings, but this does bias the results toward models with larger ensembles. The full list of CMIP models considered in this study is provided in Table S2 of Supporting Information S1.

2.4. Model Resolution and Sea Ice Analysis

Following Rackow et al. (2022), we define the nominal Southern Ocean model grid spacing as the square root of the grid cell area, averaged over the latitude band 45°S–65°S. For the GFDL model hierarchy, the Southern Ocean grid spacings are 8, 16, 31, and 62 km for the 1/8°, 1/4°, 1/2°, and 1° ocean components, respectively. For the NCAR model hierarchy, the Southern Ocean grid spacings are 6 and 66 km, for the 1/10° and 1° ocean components, respectively. Ocean resolution has progressively increased across CMIP generations. The CMIP3 models have Southern Ocean grid spacings that range from 67 to 390 km with a median grid spacing of 102 km. CMIP5 and CMIP6 models feature higher Southern Ocean resolutions that range from 35 to 126 km with median of 84 km in CMIP5 and from 16 to 94 km with a median of 63 km in CMIP6.

The Rossby radius of deformation in the Southern Ocean is approximately 13 km (Rackow et al., 2022), thus a model resolution of roughly 6.5 km is required to be considered "eddy resolving" in this region (Hallberg, 2013). Therefore, the CESM-HR model reaches the threshold of being eddy resolving in the Southern Ocean. The highest resolution GFDL model, CM4X-p125, is "eddy permitting," as its 8 km resolution satisfies $0.5R < r < R$, where r is the grid spacing and R is the Rossby radius. All other models in this study have $r > R$.

Atmospheric model resolution has also increased across CMIP generations. The atmospheric grid spacings over the Southern Ocean span 95–388 km in CMIP3 (median 240 km), 63–319 km in CMIP5 (median 159 km), and 42–242 km in CMIP6 (median 95 km). The GFDL model hierarchy contains models with atmospheric grid spacings of 24, 48, and 96 km, respectively, over the Southern Ocean region. The CESM-HR and CESM-LR have Southern Ocean grid spacings of 21 and 84 km, respectively.

We assess the models using the NOAA/NSIDC climate data record (CDR) of sea ice concentration (SIC), version 6 (G02202; Meier et al. (2021)), which is provided on the 25-km NSIDC polar stereographic south grid and spans the period 1979–2025. Antarctic SIE is the area integral of all Southern Hemisphere grid cells covered by at least 15% SIC. Antarctic SIA is the Southern Hemisphere area integral of SIC. We assess the statistical significance of ensemble-mean trends using a bootstrapping approach in which the ensemble is repeatedly resampled (with replacement) to produce an empirical distribution of ensemble-mean trends based on 1000 realizations. The significance of ensemble-mean trend differences between two ensembles is evaluated by adding the standard errors of ensemble-mean trends in quadrature to obtain a standard error for the trend difference. If the trend difference exceeds 1.96 standard errors, it is considered statistically significant at the 95% confidence level.

3. Model Resolution and Antarctic SIE Trends in CMIP Models

3.1. Ocean Resolution

Rackow et al. (2022) found a notable negative correlation between Antarctic September SIE trends and ocean grid spacing across a group of 26 CMIP5 models (see their Figure 1). Specifically, when a model selection criterion was applied based on the agreement of simulated climatological SIE with observations, Rackow et al. (2022) found a statistically significant negative correlation of $r = -0.63$ $(r^2 = 0.40)$ based on the selected subgroup of 15 models. When all 26 CMIP5 models were included, the correlation was reduced to $r = -0.33$ $(r^2 = 0.11)$. Here, we revisit this finding using CMIP3, CMIP5, and CMIP6 models. Exploring these three generations of CMIP models allows us to probe a wider range of model resolutions, since CMIP6 models were generally higher resolution than CMIP5 models, whereas CMIP3 models were generally lower resolution. This also allows us to examine the relationship between Antarctic SIE trends and ocean resolution across a much larger number of models (90 total). We focus on SIE trends, but the findings are unchanged if SIA is used (see Figure S2 in Supporting Information S1).

Figure 1 shows the relationships between September (winter maximum) Antarctic SIE trends and mean September SIE, ocean grid spacing, and atmospheric grid spacing, respectively, for CMIP6, CMIP5, and CMIP3 models. Interestingly, we find that CMIP6 models do not display a clear relationship between September SIE trends and ocean resolution (Figure 1b). In particular, the set of all CMIP6 models has a weak positive correlation with ocean resolution of $r_{all} = 0.15$ $(r_{all}^2 = 0.04)$. We also apply the model selection criterion of Rackow

19448007, 2026, 16, Downloaded from https://agupubs.onlinelibrary.wiley.com/doi/10.1029/2026GL124043, Wiley Online Library on [20/08/2026]. See the Terms and Conditions (https://onlinelibrary.wiley.com/terms-and-conditions) on Wiley Online Library for rules of use; OA articles are governed by the applicable Creative Commons License

10.1029/2026GL124043

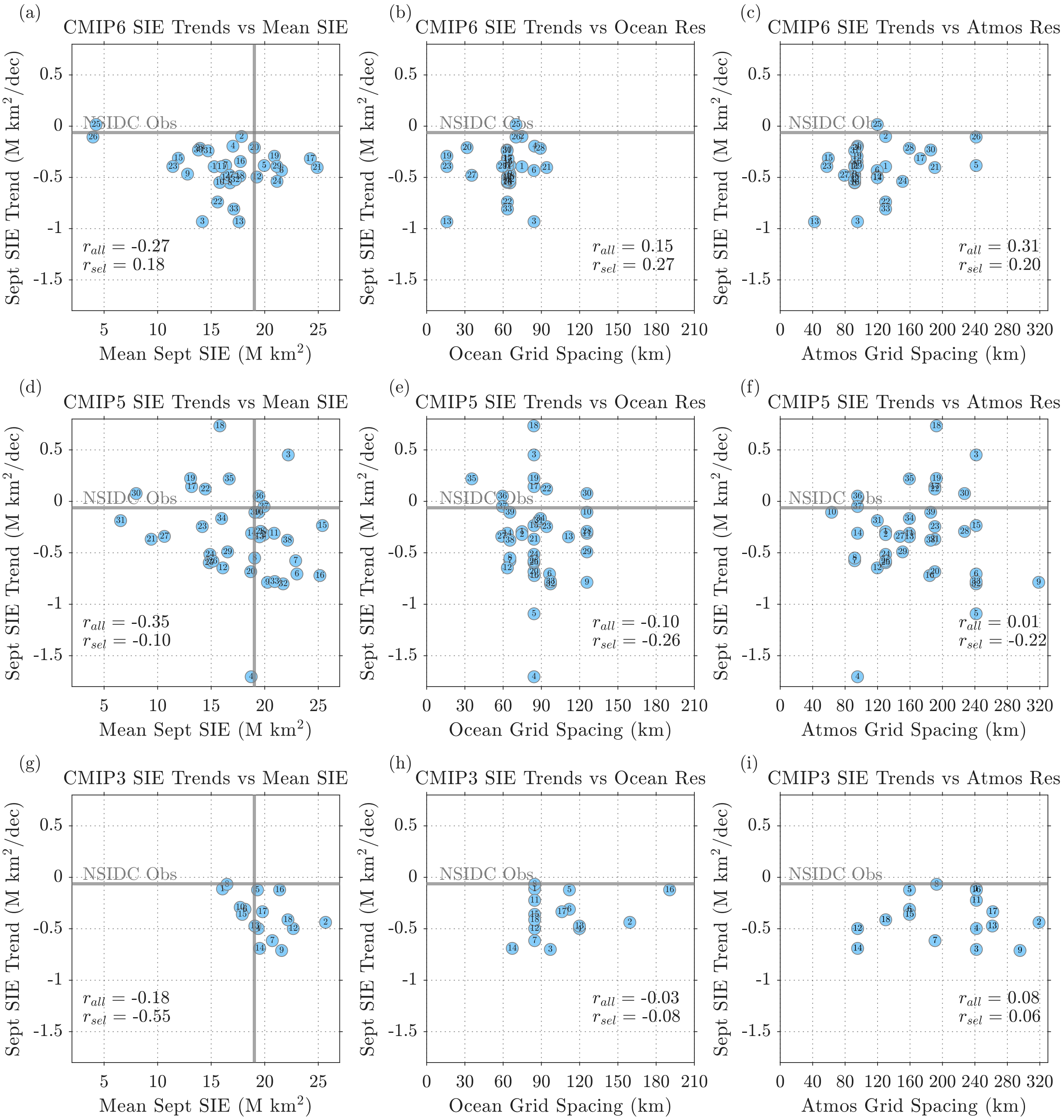

Figure 1. Relationships between September Antarctic SIE trends over the period 1979–2025 and mean September SIE (left column), ocean grid spacing (middle column), and atmospheric grid spacing (right column) for CMIP6 (a–c), CMIP5 (d–f), and CMIP3 (g–i) models. The horizontal and vertical gray lines indicate the NSIDC observed trend and mean SIE values, respectively. Correlations are computed over the set of all models in each panel (r_{all}) as well as over a selected subset of models, whose mean September SIE is within 3 million km^2 of the observed value (r_{sel}) following Rackow et al. (2022). The CMIP model numbers are indicated within the blue markers and their names are provided in Table S2 of Supporting Information S1.

et al. (2022), which considers models whose mean September SIE is within 3 million km^2 of the observed value. This selected subset of models (18 of the 33 CMIP6 models) has a slightly larger positive correlation of $r_{sel} = 0.27$ ($r_{sel}^2 = 0.07$). In either case, the CMIP6 models do not display the negative correlation that Rackow et al. (2022) identified in CMIP5 models.

19448007, 2026, 16, Downloaded from https://agupubs.onlinelibrary.wiley.com/doi/10.1029/2026GL124043, Wiley Online Library on [20/08/2026]. See the Terms and Conditions (https://onlinelibrary.wiley.com/terms-and-conditions) on Wiley Online Library for rules of use; OA articles are governed by the applicable Creative Commons License

We also revisit this relationship in CMIP5 models, expanding to a larger group of models (38 vs. 26) and a slightly longer time period (1979–2025 vs. 1979–2018) than those considered in Rackow et al. (2022). We find that the relationship between ocean resolution and SIE trends largely disappears when this larger set of models is analyzed (Figure 1e). We find a weak negative correlation for both the full set of models ($r_{all} = -0.10$; 38 models) as well as the selected models ($r_{sel} = -0.26$; 19 models). These correlation values are also reduced relative to Rackow et al. (2022) due to ocean resolution values being reported incorrectly for six models that provide their sea ice output on the atmosphere grid. Similarly, we find no clear relationship between SIE trends and ocean model resolution in CMIP3 models (Figure 1h), which have correlation values of $r_{all} = -0.03$ and $r_{sel} = -0.08$ for the full and selected sets of models, respectively. Considering other months of the year, we find that the correlation values are generally small across all months of the year, and do not display a consistent sign across CMIP generations (see Figures S1a–S1c in Supporting Information S1). Overall, these results suggest that there is no robust relationship between ocean model resolution and Antarctic SIE trends in CMIP3, CMIP5, and CMIP6 models. In fact, even if resolved eddies would systematically affect simulated trends (further explored below), one would not expect this influence to be evident within the CMIP resolution range ($r > R$), adding plausibility to the lack of relationship found here.

3.2. Atmosphere Resolution

Next, we consider the relationship between atmospheric model resolution and Antarctic SIE trends. Atmospheric model resolution could impact simulated sea ice in a number of ways, including via the position of the midlatitude eddy-driven Southern Hemisphere jet, the variability of the Southern Annular Mode, the representation of Antarctic katabatic winds, the representation of the Southern Ocean Ekman-driven cell, and coupled climate feedbacks associated with differences in the aerosol indirect effect (Barthélemy et al., 2012; Bracegirdle et al., 2020; Chen et al., 2025; Mathiot et al., 2010; Zhao et al., 2018b). Across the three generations of CMIP models, we find no clear relationship between atmospheric model grid spacing and September Antarctic SIE trends (Figures 1c, 1f, and 1i). This is also the case for other months of the year (Figures S1d–S1f in Supporting Information S1). The CMIP6 models show a consistent weak positive correlation between Antarctic SIE trends and atmospheric grid spacing in all months of the year, with correlation values ranging from $0.02 < r_{all} < 0.35$ across the full set of models. The CMIP5 and CMIP3 models lack a consistent correlation sign across months, and the correlation magnitudes are small (less than 0.2) for most months of the year. Overall, similar to the ocean resolution results, our findings suggest that there is no robust relationship between atmospheric model resolution and Antarctic SIE trends across CMIP3, CMIP5, and CMIP6 models.

4. Antarctic SIE Trends Across Two High-Resolution Model Hierarchies

We next consider the GFDL and NCAR model resolution hierarchies, which each include models that exceed the highest resolution oceanic and atmospheric components in CMIP6. Figures 2a and 2c show time series of September Pan-Antarctic SIE across the model hierarchies (colors) and in observations (black). Figures 2b and 2d plot the corresponding linear trends of these time series, computed between 1979 and different end years ranging from 2010 to 2100. For example, the observational trend in Figure 2b shows that the September Antarctic SIE trend was positive in 2010, reached a maximum positive value in 2014, and then began to approach near-zero values during the recent low SIE years from 2015 to present.

We find that the SIE trends across the GFDL and NCAR models have a large spread, which reduces as the considered trend period becomes longer. Notably, even 47-year trends computed over 1979–2025 display large contributions from internal variability, especially in certain models. In particular, SPEAR_LO (magenta), SPEAR_MED (cyan), and CESM-HR (purple) are characterized by large amplitude multi-decadal internal variability. These models display a wide distribution of trends, including members with both positive and strongly negative trends. Selected SPEAR_LO ensemble members maintain positive SIE trends beyond the year 2040. For all models, the ensemble-mean trends are consistently negative, and become more negative over the course of the 21st century.

In the GFDL model hierarchy, we find that the high-resolution CM4X-p125 model with 1/8° ocean resolution (blue) shows no evidence of a delayed sea ice decline relative to the low-resolution model counterparts (Figure 2b). CM4X-p125 rather shows simulated sea ice trends that are on the negative end of the multi-model

19448007, 2026, 16, Downloaded from https://agupubs.onlinelibrary.wiley.com/doi/10.1029/2026GL124043, Wiley Online Library on [20/08/2026]. See the Terms and Conditions (https://onlinelibrary.wiley.com/terms-and-conditions) on Wiley Online Library for rules of use; OA articles are governed by the applicable Creative Commons License

10.1029/2026GL124043

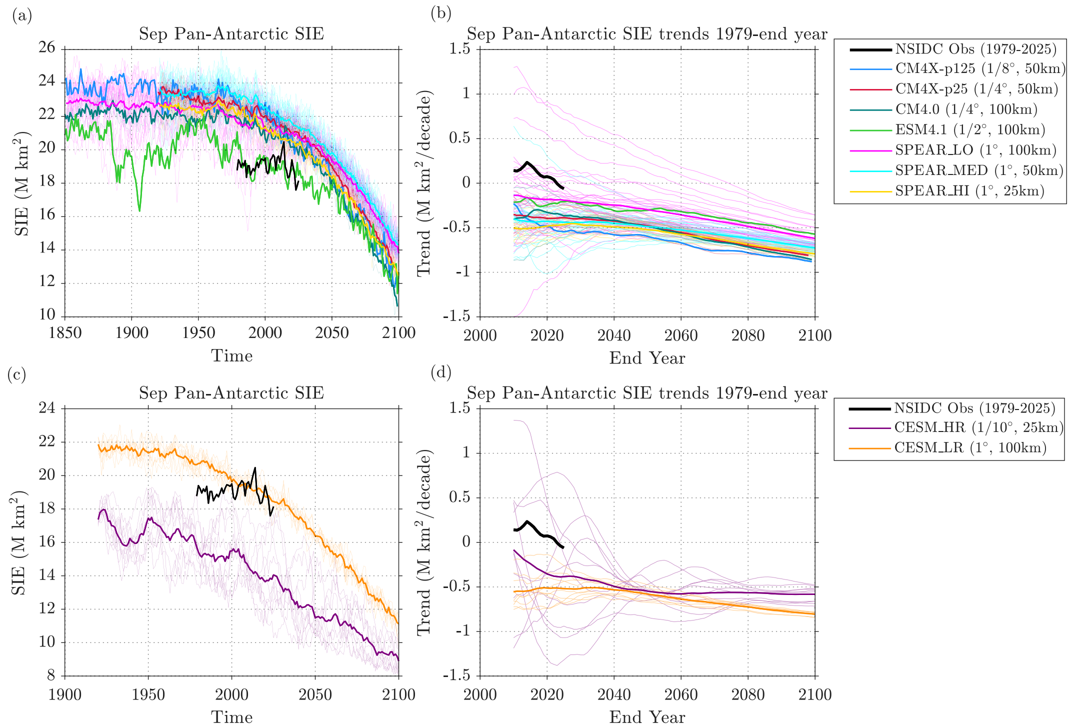

Figure 2. (a) September Pan-Antarctic SIE time series for the GFDL model hierarchy (colors) and NSIDC observations (black). The thin lines are ensemble members and the solid lines are ensemble means; (b) September Pan-Antarctic SIE trends computed between 1979 and different end years from 2010 to 2100. The GFDL model hierarchy is plotted in colors and NSIDC observations are plotted in black. Panels (c, d) show the same as (a, b) but for the NCAR model resolution hierarchy. The nominal oceanic and atmospheric resolutions are indicated in parentheses in the legend.

SIE trend distribution. Similarly, the models with 1/4° ocean components, CM4X-p25 (red) and CM4.0 (turquoise), do not show evidence of a delayed sea ice decline.

In the NCAR model hierarchy, the ensemble mean of CESM-HR has less negative trends than the ensemble mean of CESM-LR over the period 2010–2040 (Figure 2d). However, the ensemble-mean trend differences over this period are not statistically significant due to the large trend variability within CESM-HR. It is also notable that the ensemble-mean of CESM-HR displays synchronized multi-decadal variability, indicating some memory of initial conditions across the ensemble. This is likely due to the fact that the CESM-HR and CESM-LR ensembles are generated using "micro-perturbations" (Castruccio et al., 2024; Deser et al., 2020), in which members are initialized from the same phase of internal climate variability with round-off level perturbations to the atmospheric initial conditions. The coherent phasing of multi-decadal variability in CESM-HR can be seen in the ensemble-mean trends shown in Figure 2d and contributes to the less negative trend values that occur for end-years near 2010. Over the late 21st century, the ensemble-mean of CESM-HR has less negative trends than CESM-LR, and these ensemble-mean trend differences are statistically significant over the period 2069–2100. This difference in late 21st century trends is likely related to the large differences in SIE mean state in the late 20th century. For example, the CMIP ensembles show that models with larger SIE mean state over 1979–1998 tend to have more negative SIE trends over the period 1979–2090 (correlations for September SIE are −0.46, −0.59, and 0.00 for CMIP6, CMIP5, and CMIP3, respectively).

In Figure 3, we examine the relationship between SIE trends and model resolution more closely. Given the demonstrated large contributions of internal variability to 47-year trends, it is important to account for internal variability uncertainty in models with only a single member. We do this by computing a probability distribution function of 47-year SIE trends using a 500-year pre-industrial control simulation, from which we estimate a 95% confidence interval. Figure 3a shows a scatterplot of September Antarctic SIE trends over 1979–2025 versus ocean model grid spacing. We find that there is no clear relationship between SIE trends and ocean grid spacing across the high-resolution model hierarchies. The eddy-resolving and eddy-permitting ocean models, CESM-HR

19448007, 2026, 16, Downloaded from https://agupubs.onlinelibrary.wiley.com/doi/10.1029/2026GL124043, Wiley Online Library on [20/08/2026]. See the Terms and Conditions (https://onlinelibrary.wiley.com/terms-and-conditions) on Wiley Online Library for rules of use; OA articles are governed by the applicable Creative Commons License

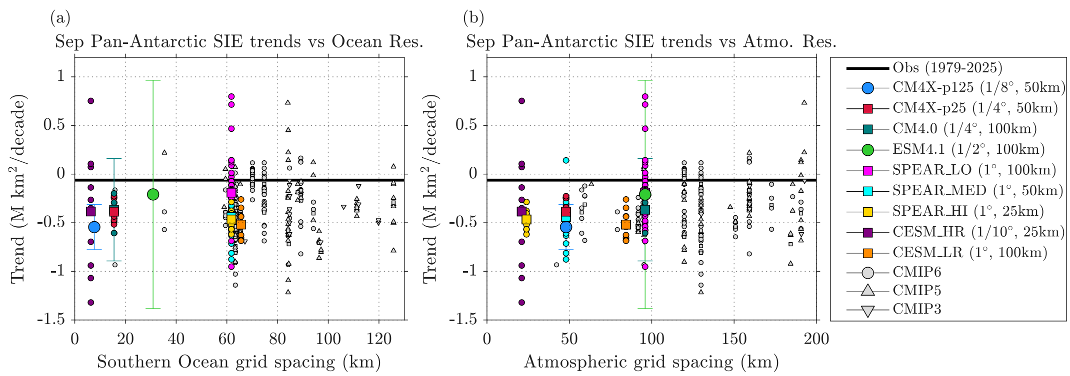

Figure 3. Relationship between ocean and atmosphere model grid spacing and September Antarctic SIE trends over 1979–2025 across the GFDL and NCAR model hierarchies. Circle markers indicate ensemble members and squares indicate the ensemble mean. For models with three or fewer members, 47-year trend uncertainty is estimated using a PI control simulation and the error bars indicate a 95% confidence interval. CMIP model ensemble members are shown in gray markers. For CMIP models with 3 or more members, their ensemble mean is plotted as a gray square.

and CM4X-p125, do not show evidence of a delayed SIE decline. This differs from the main finding of Rackow et al. (2022), who documented a delayed decline in a high-resolution configuration with 14 km Southern Ocean grid spacing. We also observe large contributions of internal variability to SIE trends over 1979–2025, demonstrating the need for multiple model realizations in order to robustly attribute simulated trend differences to structural model differences.

While the high-resolution GFDL and NCAR model hierarchies are each constructed using common components, individual models within a given hierarchy differ in configuration choices, such as ocean mesoscale and sub-mesoscale eddy parameterizations. This implies that comparisons made across a given hierarchy confound resolution-based effects with structural model differences, precluding definitive conclusions about the direct impact of resolution. These confounding effects are a generic challenge for studies that compare high and low resolution counterpart models, since low-ocean resolution models rely upon eddy parameterizations to achieve credible climate simulations.

Figure 3b shows SIE trends versus atmospheric model grid spacing. Overall, there is no clear relationship between these two quantities across the model hierarchies. We do, however, find some notable relationships between trend variability and atmospheric grid spacing. In particular, within the GFDL model hierarchy, SIE trend variability tends to systematically increase as the atmospheric grid spacing increases. This is the case across the three SPEAR models, which are a "clean" hierarchy in which only the atmospheric resolution changes, as well as across the full group of GFDL models (see Figure S3 in Supporting Information S1). The 100 km atmosphere models in particular display large amplitude multi-decadal SIE variability, which leads to significantly more variability in 47-year SIE trends than their higher-atmosphere resolution counterparts (Figure S3 in Supporting Information S1). Interestingly, the NCAR models show the opposite relationship: CESM-HR with its high-resolution atmosphere has more trend variability than CESM-LR. Since both ocean and atmosphere resolution differ between the CESM HR and LR models, these differences in trend variability cannot be cleanly attributed to atmospheric resolution. However, the NCAR models clearly demonstrate that the GFDL-based finding that low-resolution atmospheres have more SIE trend variability is not generic across other models. We return to the physical drivers of this trend variability in the discussion section.

5. Discussion and Conclusions

In this work, we have investigated the question: Do high-resolution climate models improve simulated Antarctic sea ice trends? Across the high-resolution models considered here, we have found no detectable improvements associated with resolution. In particular, we found that there is no clear relationship between Antarctic SIE trends and horizontal ocean and atmosphere resolution across high-resolution hierarchies of GFDL and NCAR models, as well as across CMIP3, CMIP5, and CMIP6 models. This is the case for both the 1979–2025 satellite period and the remainder of the 21st century. Our findings differ from Rackow et al. (2022), who found a delayed SIE decline

19448007, 2026, 16, Downloaded from https://agupubs.onlinelibrary.wiley.com/doi/10.1029/2026GL124043, Wiley Online Library on [20/08/2026]. See the Terms and Conditions (https://onlinelibrary.wiley.com/terms-and-conditions) on Wiley Online Library for rules of use; OA articles are governed by the applicable Creative Commons License

19448007, 2026, 16, Downloaded from https://agupubs.onlinelibrary.wiley.com/doi/10.1029/2026GL124043, Wiley Online Library on [20/08/2026]. See the Terms and Conditions (https://onlinelibrary.wiley.com/terms-and-conditions) on Wiley Online Library for rules of use; OA articles are governed by the applicable Creative Commons License

in a high-resolution ocean model, suggesting that the relationship between Antarctic sea ice trends and ocean resolution is likely model-dependent, and is also likely obscured by internal climate variability.

A key finding of this work is that internal variability makes large contributions to Antarctic SIE trends over the period 1979–2025, and that spurious relationships to model resolution could be identified if only single model realizations were considered. We find that the models capable of capturing observed SIE trends with particular ensemble members are those that exhibit large amplitude multi-decadal Southern Ocean climate variability. This is the case with CESM-HR, SPEAR_LO, and SPEAR_MED. We also expect that ESM4.1 and CM4.0 would exhibit trend agreement for certain realizations, if additional ensemble members were available. Other models, specifically CM4X-p125, CM4X-p25, SPEAR_HI, and CESM_LR, have smaller amplitude trend variability (Figure S3 in Supporting Information S1) and do not have members that agree with observed trends. Given that large amplitude multi-decadal SIE variability appears to be a necessary condition for capturing observed SIE trends, a crucial question is: Is this variability realistic?

The unifying simulation feature that drives multi-decadal variability across these models is Southern Ocean deep convective variability associated with open-ocean polynyas in the Weddell or Ross Seas (Beadling et al., 2022; Chang et al., 2020; Chen et al., 2026; Diao et al., 2022; Dunne et al., 2020; Ford & Rose, 2026; Held et al., 2019; Tesdal et al., 2023; Zhang et al., 2019, 2021). This deep convective variability is directly linked to SIE variability via a charge-discharge mechanism, in which an oceanic subsurface reservoir slowly accumulates heat over multiple decades (the charge phase) until the water column convectively destabilizes, leading to deeper mixed layers, increased vertical mixing of subsurface heat, and increased basal sea ice melt (the discharge phase). This unifying feature is also present in recent work by Zapponini et al. (2026). Using a high-resolution AWI model that is eddy-permitting over the Antarctic Circumpolar Current, they found that their high-resolution configuration exhibited large multi-decadal SIE variability that was not present in a low-resolution counterpart. They showed that this variability is associated with Weddell Sea polynya variability, and leads to a stable SIE cover over the satellite period followed by an abrupt decline around 2030.

While open-ocean Weddell Sea polynyas have been observed in the mid-1970s (Carsey, 1980) and 2016–17 (Campbell et al., 2019), the polynya events simulated by models may be too large; however, uncertainties in current ice-core-based polynya reconstructions preclude precise statements on this point (Goosse et al., 2021). We also note that while some model ensemble members capture near-zero Pan-Antarctic SIE trends (e.g., CESM-HR members 6, 7, 10 and SPEAR_LO members 7, 10, 18, and 19), these members do not have the correct spatial patterns of SIC trends (see Figures S4–S6 in Supporting Information S1). Specifically, these members have large SIC trend features in the Weddell and Ross Seas, which are not present in observations, suggesting that they are getting the "right answer for the wrong reasons."

While this study has not identified a clear connection between ocean and atmosphere resolution and Antarctic SIE trends, future work on this topic is needed, especially multi-model assessments of eddy-resolving simulations in the Southern Ocean. A persistent challenge is that studies at frontier resolutions can often only afford to run a single ensemble member and a relatively short control integration (e.g., Kang et al., 2026). This work emphasizes that single-member studies are inherently limited in their ability to quantify structural model differences and resolution-dependent climate signals, and that ensembles should be prioritized whenever computationally feasible.

Conflict of Interest

The authors declare no conflicts of interest relevant to this study.

Availability Statement

Data for all models and code to analyze data and make figures are available via an online repository (Bushuk et al., 2026). The CMIP3, CMIP5, and CMIP6 data used for this study are publicly available from the Earth System Grid Federation (ESGF). The CESM-HR and CESM-LR data are available through the NSF NCAR Geoscience Data Exchange (GDEX; https://gdex.ucar.edu/datasets) platform (data sets d651007, d651009, and d651030). The NSIDC CDR SIC data are available from the NSIDC data portal (https://nsidc.org/data/g02202).

19448007, 2026, 16, Downloaded from https://agupubs.onlinelibrary.wiley.com/doi/10.1029/2026GL124043, Wiley Online Library on [20/08/2026]. See the Terms and Conditions (https://onlinelibrary.wiley.com/terms-and-conditions) on Wiley Online Library for rules of use; OA articles are governed by the applicable Creative Commons License

Acknowledgments

We thank two anonymous reviewers for insightful comments that improved the manuscript. We thank Mike Winton for many stimulating discussions which helped to shape this work. We thank John Krasting and Youngji Joh for valuable comments on a preliminary draft of this manuscript. We thank Dirk Notz and Stefan Kern for making CMIP6 processed sea ice area data publicly available and for also sharing CMIP6 model grid information. We thank Lettie Roach for making CMIP5 processed sea ice area data publicly available. We thank Andrew Roberts and Evgeny Volodin for assistance with the E3SMv1 and INM-CM model grids, respectively. We thank Jan-Erik Tesdal and John Krasting for sharing data from two additional CM4.0 ensemble members. This research was supported through base funding from NOAA to the GFDL. D.B.B. was supported by the Cooperative Institute for Climate, Ocean, & Ecosystem Studies (CICOES) under NOAA Cooperative Agreement NA20OAR4320271, Contribution No. 2026–1539. S.M.G. is funded through the France 2030 Choose France for Science program implemented by ANR (Agence Nationale de la Recherche) through CNRS at IPSL/LOCEAN (UMR7159, CNRS-IRD- MNHN-Sorbonne Université) in Paris. Y.-T.C. is supported by award NA23OAR4320198 from the National Oceanic and Atmospheric Administration, U.S. Department of Commerce.

References

Abram, N. J., Purich, A., England, M. H., McCormack, F. S., Strugnell, J. M., Bergstrom, D. M., et al. (2025). Emerging evidence of abrupt changes in the Antarctic environment. *Nature*, *644*(8077), 621–633. https://doi.org/10.1038/s41586-025-09349-5

Adcroft, A., Anderson, W., Balaji, V., Blanton, C., Bushuk, M., Dufour, C. O., et al. (2019). The GFDL global ocean and sea ice model OM4.0: Model description and simulation features. *Journal of Advances in Modeling Earth Systems*, *11*(10), 3167–3211. https://doi.org/10.1029/2019MS001726

Armour, K. C., Marshall, J., Scott, J. R., Donohoe, A., & Newsom, E. R. (2016). Southern Ocean warming delayed by circumpolar upwelling and equatorward transport. *Nature Geoscience*, *9*(7), 549–554. https://doi.org/10.1038/ngeo2731

Barthélemy, A., Goosse, H., Mathiot, P., & Fichefet, T. (2012). Inclusion of a katabatic wind correction in a coarse-resolution global coupled climate model. *Ocean Modelling*, *48*, 45–54. https://doi.org/10.1016/j.ocemod.2012.03.002

Beadling, R., Krasting, J., Griffies, S., Hurlin, W., Bronselaer, B., Russell, J., et al. (2022). Importance of the Antarctic Slope Current in the Southern Ocean response to ice sheet melt and wind stress change. *Journal of Geophysical Research: Oceans*, *127*(5), e2021JC017608. https://doi.org/10.1029/2021JC017608

Bilgen, S. I., & Kirtman, B. P. (2020). Impact of ocean model resolution on understanding the delayed warming of the Southern Ocean. *Environmental Research Letters*, *15*(11), 114012. https://doi.org/10.1088/1748-9326/abbc3e

Bitz, C., & Polvani, L. M. (2012). Antarctic climate response to stratospheric ozone depletion in a fine resolution ocean climate model. *Geophysical Research Letters*, *39*(20). https://doi.org/10.1029/2012GL053393

Bracegirdle, T., Holmes, C., Hosking, J., Marshall, G., Osman, M., Patterson, M., & Rackow, T. (2020). Improvements in circumpolar Southern Hemisphere extratropical atmospheric circulation in CMIP6 compared to CMIP5. *Earth and Space Science*, *7*(6), e2019EA001065. https://doi.org/10.1029/2019EA001065

Bronselaer, B., Winton, M., Griffies, S. M., Hurlin, W. J., Rodgers, K. B., Sergienko, O. V., et al. (2018). Change in future climate due to Antarctic meltwater. *Nature*, *564*(7734), 53–58. https://doi.org/10.1038/s41586-018-0712-z

Bushuk, M., Bonan, D. B., Griffies, S. M., Gregory, W., Zhang, Y., Hurlin, B., et al. (2026). Data and code for "Historical and projected Antarctic sea ice trends across high-resolution coupled model hierarchies". *Zenodo*. https://doi.org/10.5281/zenodo.19740836

Campbell, E. C., Wilson, E. A., Moore, G. K., Riser, S. C., Brayton, C. E., Mazloff, M. R., & Talley, L. D. (2019). Antarctic offshore polynyas linked to Southern Hemisphere climate anomalies. *Nature*, *570*(7761), 319–325. https://doi.org/10.1038/s41586-019-1294-0

Carsey, F. (1980). Microwave observation of the Weddell Polynya. *Monthly Weather Review*, *108*(12), 2032–2044. https://doi.org/10.1175/1520-0493(1980)108⟨2032:MOOTWP⟩2.0.CO;2

Castruccio, F., Chang, P., Danabasoglu, G., Fu, D., Rosenbloom, N., Zhang, Q., et al. (2024). *MESACLIP: A 10-member ensemble of CESM HR historical (1920-2005) simulations*. NSF National Center for Atmospheric Research. https://doi.org/10.5065/7N1X-K278

Chang, P., Zhang, S., Danabasoglu, G., Yeager, S. G., Fu, H., Wang, H., et al. (2020). An unprecedented set of high-resolution earth system simulations for understanding multiscale interactions in climate variability and change. *Journal of Advances in Modeling Earth Systems*, *12*(12), e2020MS002298. https://doi.org/10.1029/2020MS002298

Chassignet, E. P., Yeager, S. G., Fox-Kemper, B., Bozec, A., Castruccio, F., Danabasoglu, G., et al. (2020). Impact of horizontal resolution on global ocean–sea ice model simulations based on the experimental protocols of the Ocean Model Intercomparison Project phase 2 (OMIP-2). *Geoscientific Model Development*, *13*(9), 4595–4637. https://doi.org/10.5194/gmd-13-4595-2020

Chen, T.-C., Goosse, H., Davrinche, C., Libera, S., Roberts, C., Aengenheyster, M., et al. (2025). Southern Annular Mode persistence and westerly jet: A reassessment using high-resolution global models. *Weather and Climate Dynamics*, *6*(4), 1179–1193. https://doi.org/10.5194/wcd-6-1179-2025

Chen, Y.-T., Merlis, T. M., Dinh, T., Griffies, S. M., Krasting, J. P., Dussin, R., et al. (2026). Assessing Earth's energy imbalance trend in the early 21st century in two high-resolution coupled models. *Geophysical Research Letters*, *53*(9), e2025GL121277. https://doi.org/10.1029/2025GL121277

Danabasoglu, G., Bates, S. C., Briegleb, B. P., Jayne, S. R., Jochum, M., Large, W. G., et al. (2012). The CCSM4 ocean component. *Journal of Climate*, *25*(5), 1361–1389. https://doi.org/10.1175/JCLI-D-11-00091.1

Delworth, T. L., Cooke, W. F., Adcroft, A., Bushuk, M., Chen, J.-H., Dunne, K. A., et al. (2020). SPEAR: The next generation GFDL modeling system for seasonal to multidecadal prediction and projection. *Journal of Advances in Modeling Earth Systems*, *12*(3), e2019MS001895. https://doi.org/10.1029/2019MS001895

Deser, C., Lehner, F., Rodgers, K., Ault, T., Delworth, T., DiNezio, P., et al. (2020). Insights from Earth system model initial-condition large ensembles and future prospects. *Nature Climate Change*, *10*(4), 277–286. https://doi.org/10.1038/s41558-020-0731-2

Dhame, S., Olonscheck, D., & Rugenstein, M. (2025). Higher-resolution climate models do not consistently reproduce the observed tropical Pacific warming pattern. *Journal of Climate*, *38*(13), 3131–3149. https://doi.org/10.1175/JCLI-D-24-0248.1

Diao, X., Stössel, A., Chang, P., Danabasoglu, G., Yeager, S. G., Gopal, A., et al. (2022). On the intermittent occurrence of open-Ocean Polynyas in a multi-century high-resolution preindustrial earth system model simulation. *Journal of Geophysical Research: Oceans*, *127*(4), e2021JC017672. https://doi.org/10.1029/2021jc017672

Doddridge, E. W., Marshall, J., Song, H., Campin, J.-M., Kelley, M., & Nazarenko, L. (2019). Eddy compensation dampens Southern Ocean sea surface temperature response to westerly wind trends. *Geophysical Research Letters*, *46*(8), 4365–4377. https://doi.org/10.1029/2019GL082758

Dunne, J., Horowitz, L., Adcroft, A., Ginoux, P., Held, I., John, J., et al. (2020). The GFDL Earth System Model version 4.1 (GFDL-ESM 4.1): Overall coupled model description and simulation characteristics. *Journal of Advances in Modeling Earth Systems*, *12*(11), e2019MS002015. https://doi.org/10.1029/2019MS002015

Eyring, V., Bony, S., Meehl, G. A., Senior, C. A., Stevens, B., Stouffer, R. J., & Taylor, K. E. (2016). Overview of the Coupled Model Intercomparison Project Phase 6 (CMIP6) experimental design and organization. *Geoscientific Model Development*, *9*(5), 1937–1958. https://doi.org/10.5194/gmd-9-1937-2016

Ferreira, D., Marshall, J., Bitz, C. M., Solomon, S., & Plumb, A. (2015). Antarctic Ocean and sea ice response to ozone depletion: A two-timescale problem. *Journal of Climate*, *28*(3), 1206–1226. https://doi.org/10.1175/JCLI-D-14-00313.1

Fogt, R. L., Sleinkofer, A. M., Raphael, M. N., & Handcock, M. S. (2022). A regime shift in seasonal total Antarctic sea ice extent in the twentieth century. *Nature Climate Change*, *12*(1), 54–62. https://doi.org/10.1038/s41558-021-01254-9

Ford, R. R., & Rose, B. E. (2026). A Southern Ocean multidecadal oscillator forced by deep convection. *Geophysical Research Letters*, *53*(6), e2025GL120643. https://doi.org/10.1029/2025GL120643

Goosse, H., Dalaiden, Q., Cavitte, M. G., & Zhang, L. (2021). Can we reconstruct the formation of large open-ocean polynyas in the Southern Ocean using ice core records? *Climate of the Past*, *17*(1), 111–131. https://doi.org/10.5194/cp-17-111-2021

Griffies, S. M., Adcroft, A., Beadling, R., Bushuk, M., Chang, C.-Y., Drake, H., et al. (2025a). The GFDL-CM4X climate model hierarchy, Part II: Case studies. *Journal of Advances in Modeling Earth Systems*, *17*(10), e2024MS004862. https://doi.org/10.1029/2024MS004862

Griffies, S. M., Adcroft, A., Beadling, R., Bushuk, M., Chang, C.-Y., Drake, H., et al. (2025b). The GFDL-CM4X climate model hierarchy, Part I: Model description and thermal properties. *Journal of Advances in Modeling Earth Systems*, *17*(10), e2024MS004861. https://doi.org/10.1029/2024MS004861

Haarsma, R. J., Roberts, M. J., Vidale, P. L., Senior, C. A., Bellucci, A., Bao, Q., et al. (2016). High resolution model intercomparison project (HighResMIP v1. 0) for CMIP6. *Geoscientific Model Development*, *9*(11), 4185–4208. https://doi.org/10.5194/gmd-9-4185-2016

Hallberg, R. (2013). Using a resolution function to regulate parameterizations of oceanic mesoscale eddy effects. *Ocean Modelling*, *72*, 92–103. https://doi.org/10.1016/j.ocemod.2013.08.007

Hallberg, R., & Gnanadesikan, A. (2006). The role of eddies in determining the structure and response of the wind-driven Southern Hemisphere overturning: Results from the modeling Eddies in the Southern Ocean (MESO) project. *Journal of Physical Oceanography*, *36*(12), 2232–2252. https://doi.org/10.1175/JPO2980.1

Held, I., Guo, H., Adcroft, A., Dunne, J., Horowitz, L., Krasting, J., et al. (2019). Structure and performance of GFDL's CM4. 0 climate model. *Journal of Advances in Modeling Earth Systems*, *11*(11), 3691–3727. https://doi.org/10.1029/2019MS001829

Hobbs, W., Spence, P., Meyer, A., Schroeter, S., Fraser, A. D., Reid, P., et al. (2024). Observational evidence for a regime shift in summer Antarctic sea ice. *Journal of Climate*, *37*(7), 2263–2275. https://doi.org/10.1175/JCLI-D-23-0479.1

Hogg, A. M. C., Meredith, M. P., Blundell, J. R., & Wilson, C. (2008). Eddy heat flux in the Southern Ocean: Response to variable wind forcing. *Journal of Climate*, *21*(4), 608–620. https://doi.org/10.1175/2007JCLI1925.1

Holland, P. R., & Kwok, R. (2012). Wind-driven trends in Antarctic sea-ice drift. *Nature Geoscience*, *5*(12), 872–875. https://doi.org/10.1038/ngeo1627

Holmes, C. R., Bracegirdle, T. J., Holland, P. R., Stroeve, J., & Wilkinson, J. (2024). Brief communication: New perspectives on the skill of modelled sea ice trends in light of recent Antarctic sea ice loss. *The Cryosphere*, *18*(12), 5641–5652. https://doi.org/10.5194/tc-18-5641-2024

Hunke, E., Lipscomb, W., Turner, A., Jeffery, N., & Elliott, S. (2008). *CICE: The Los Alamos sea ice model, documentation and software, version 4.0*. (Tech. Rep.). Los Alamos National Laboratory.

Kang, S. M., Putrasahan, D. A., Brizuela, N. G., Haak, H., Kröger, J., Marotzke, J., et al. (2026). Km-scale coupled simulation and model–observation SST trend discrepancy. *Proceedings of the National Academy of Sciences*, *123*(8), e2522161123. https://doi.org/10.1073/pnas.2522161123

Lawrence, D. M., Oleson, K. W., Flanner, M. G., Thornton, P. E., Swenson, S. C., Lawrence, P. J., et al. (2011). Parameterization improvements and functional and structural advances in version 4 of the Community Land Model. *Journal of Advances in Modeling Earth Systems*, *3*(1). https://doi.org/10.1029/2011MS00045

Mathiot, P., Barnier, B., Gallée, H., Molines, J. M., Le Sommer, J., Juza, M., & Penduff, T. (2010). Introducing katabatic winds in global ERA40 fields to simulate their impacts on the Southern Ocean and sea-ice. *Ocean Modelling*, *35*(3), 146–160. https://doi.org/10.1016/j.ocemod.2010.07.001

Meehl, G. A., Arblaster, J. M., Bitz, C. M., Chung, C. T., & Teng, H. (2016). Antarctic sea-ice expansion between 2000 and 2014 driven by tropical Pacific decadal climate variability. *Nature Geoscience*, *9*(8), 590–595. https://doi.org/10.1038/ngeo2751

Meehl, G. A., Yang, D., Arblaster, J. M., Bates, S. C., Rosenbloom, N., Neale, R., et al. (2019). Effects of model resolution, physics, and coupling on Southern Hemisphere storm tracks in CESM1. 3. *Geophysical Research Letters*, *46*(21), 12408–12416. https://doi.org/10.1029/2019GL084057

Meier, W. N., Fetterer, F., Windnagel, A. K., & Stewart, S. (2021). *NOAA/NSIDC Climate Data Record of passive microwave sea ice concentration, version 6*. National Snow and Ice Data Center. https://doi.org/10.7265/b18j-z797

Meinshausen, M., Smith, S. J., Calvin, K., Daniel, J. S., Kainuma, M. L., Lamarque, J.-F., et al. (2011). The RCP greenhouse gas concentrations and their extensions from 1765 to 2300. *Climatic Change*, *109*(1), 213–241. https://doi.org/10.1007/s10584-011-0156-z

Munday, D. R., Johnson, H. L., & Marshall, D. P. (2013). Eddy saturation of equilibrated circumpolar currents. *Journal of Physical Oceanography*, *43*(3), 507–532. https://doi.org/10.1175/JPO-D-12-095.1

Neale, R. B., Chen, C.-C., Gettelman, A., Lauritzen, P. H., Park, S., & Williamson, D. L. (2012). Description of the NCAR community atmosphere model (CAM 5.0). *NCAR Tech. Note Ncar/tn-486+ STR*, 1–289.

Parkinson, C. L. (2019). A 40-y record reveals gradual Antarctic sea ice increases followed by decreases at rates far exceeding the rates seen in the Arctic. *Proceedings of the National Academy of Sciences*, *116*(29), 14414–14423. https://doi.org/10.1073/pnas.1906556116

Polvani, L. M., & Smith, K. L. (2013). Can natural variability explain observed Antarctic sea ice trends? New modeling evidence from CMIP5. *Geophysical Research Letters*, *40*(12), 3195–3199. https://doi.org/10.1002/grl.50578

Purich, A., Cai, W., England, M. H., & Cowan, T. (2016). Evidence for link between modelled trends in Antarctic sea ice and underestimated westerly wind changes. *Nat. Comms.*, *7*(1), 10409. https://doi.org/10.1038/ncomms10409

Purich, A., & Doddridge, E. W. (2023). Record low Antarctic sea ice coverage indicates a new sea ice state. *Communications Earth & Environment*, *4*(1), 314. https://doi.org/10.1038/s43247-023-00961-9

Purich, A., England, M. H., Cai, W., Chikamoto, Y., Timmermann, A., Fyfe, J. C., et al. (2016). Tropical Pacific SST drivers of recent Antarctic sea ice trends. *Journal of Climate*, *29*(24), 8931–8948. https://doi.org/10.1175/JCLI-D-16-0440.1

Rackow, T., Danilov, S., Goessling, H. F., Hellmer, H. H., Sein, D. V., Semmler, T., et al. (2022). Delayed Antarctic sea-ice decline in high-resolution climate change simulations. *Nature Communications*, *13*(1), 637. https://doi.org/10.1038/s41467-022-28259-y

Raphael, M. N., Maierhofer, T. J., Fogt, R. L., Hobbs, W. R., & Handcock, M. S. (2025). A twenty-first century structural change in Antarctica's sea ice system. *Communications Earth & Environment*, *6*(1), 131. https://doi.org/10.1038/s43247-025-02107-5

Roach, L. A., Dörr, J., Holmes, C. R., Massonnet, F., Blockley, E. W., Notz, D., et al. (2020). Antarctic sea ice area in CMIP6. *Geophysical Research Letters*, *47*(9), e2019GL086729. https://doi.org/10.1029/2019GL086729

Roach, L. A., & Polvani, L. M. (2026). Persistent Antarctic sea ice biases in CMIP6 models in spite of the recent decade-long sharp decline. *Journal of Climate*, e250477. https://doi.org/10.1175/JCLI-D-25-0477.1

Schmidt, G. A., Romanou, A., Roach, L. A., Mankoff, K. D., Li, Q., Rye, C. D., et al. (2023). Anomalous meltwater from ice sheets and ice shelves is a historical forcing. *Geophysical Research Letters*, *50*(24), e2023GL106530. https://doi.org/10.1029/2023GL106530

Selivanova, J., Iovino, D., & Vichi, M. (2024). Limited benefits of increased spatial resolution for sea ice in HighResMIP simulations. *Geophysical Research Letters*, *51*(14), e2023GL107969. https://doi.org/10.1029/2023GL107969

Shu, Q., Wang, Q., Song, Z., Qiao, F., Zhao, J., Chu, M., & Li, X. (2020). Assessment of sea ice extent in CMIP6 with comparison to observations and CMIP5. *Geophysical Research Letters*, *47*(9), e2020GL087965. https://doi.org/10.1029/2020GL087965

Singh, H., Polvani, L. M., & Rasch, P. J. (2019). Antarctic sea ice expansion, driven by internal variability, in the presence of increasing atmospheric CO2. *Geophysical Research Letters*, *46*(24), 14762–14771. https://doi.org/10.1029/2019GL083758

19448007, 2026, 16, Downloaded from https://agupubs.onlinelibrary.wiley.com/doi/10.1029/2026GL124043, Wiley Online Library on [20/08/2026]. See the Terms and Conditions (https://onlinelibrary.wiley.com/terms-and-conditions) on Wiley Online Library for rules of use; OA articles are governed by the applicable Creative Commons License

Sun, S., & Eisenman, I. (2021). Observed Antarctic sea ice expansion reproduced in a climate model after correcting biases in sea ice drift velocity. *Nature Communications*, *12*(1), 1060. https://doi.org/10.1038/s41467-021-21412-z

Tesdal, J.-E., MacGilchrist, G. A., Beadling, R. L., Griffies, S. M., Krasting, J. P., & Durack, P. J. (2023). Revisiting interior water mass responses to surface forcing changes and the subsequent effects on overturning in the Southern Ocean. *Journal of Geophysical Research: Oceans*, *128*(3), e2022JC019105. https://doi.org/10.1029/2022JC019105

Turner, J., Bracegirdle, T. J., Phillips, T., Marshall, G. J., & Hosking, J. S. (2013). An initial assessment of Antarctic sea ice extent in the CMIP5 models. *Journal of Climate*, *26*(5), 1473–1484. https://doi.org/10.1175/JCLI-D-12-00068.1

Yeager, S. G., Chang, P., Danabasoglu, G., Rosenbloom, N., Zhang, Q., Castruccio, F. S., et al. (2023). Reduced Southern Ocean warming enhances global skill and signal-to-noise in an eddy-resolving decadal prediction system. *npj Climate and Atmospheric Science*, *6*(1), 107. https://doi.org/10.1038/s41612-023-00434-y

Zapponini, M., Semmler, T., Streffing, J., Rackow, T., Roach, L. A., & Jung, T. (2026). Assessing resolution sensitivity in coupled climate simulations with AWI-CM3. *EGUsphere*, *2026*(8), 1–39. https://doi.org/10.5194/gmd-19-3395-2026

Zhang, L., Delworth, T. L., Cooke, W., Goosse, H., Bushuk, M., Morioka, Y., & Yang, X. (2021). The dependence of internal multidecadal variability in the Southern Ocean on the ocean background mean state. *Journal of Climate*, *34*(3), 1061–1080. https://doi.org/10.1175/JCLI-D-20-0049.1

Zhang, L., Delworth, T. L., Cooke, W., & Yang, X. (2019). Natural variability of Southern Ocean convection as a driver of observed climate trends. *Nature Climate Change*, *9*(1), 59–65. https://doi.org/10.1038/s41558-018-0350-3

Zhao, M., Golaz, J.-C., Held, I., Guo, H., Balaji, V., Benson, R., et al. (2018a). The GFDL global atmosphere and land model AM4.0/LM4.0: 1. Simulation characteristics with prescribed SSTs. *Journal of Advances in Modeling Earth Systems*, *10*(3), 691–734. https://doi.org/10.1002/2017MS001208

Zhao, M., Golaz, J.-C., Held, I., Guo, H., Balaji, V., Benson, R., et al. (2018b). The GFDL global atmosphere and land model AM4.0/LM4.0: 2. Model description, sensitivity studies, and tuning strategies. *Journal of Advances in Modeling Earth Systems*, *10*(3), 735–769. https://doi.org/10.1002/2017MS001209

19448007, 2026, 16, Downloaded from https://agupubs.onlinelibrary.wiley.com/doi/10.1029/2026GL124043, Wiley Online Library on [20/08/2026]. See the Terms and Conditions (https://onlinelibrary.wiley.com/terms-and-conditions) on Wiley Online Library for rules of use; OA articles are governed by the applicable Creative Commons License